Anal Bioanal Chem (2006) 384: 631–637
DOI 10.1007/s00216-005-0246-8

ORIGINAL PAPER

Mikaela Nichkova · Dosi Dosev · Richard Perron · Shirley J. Gee · Bruce D. Hammock · Ian M. Kennedy

Eu^{3+}-doped Gd_2O_3 nanoparticles as reporters for optical detection and visualization of antibodies patterned by microcontact printing

Received: 8 August 2005 / Revised: 15 November 2005 / Accepted: 18 November 2005 / Published online: 14 January 2006

Abstract Lanthanide oxide nanoparticles are promising luminescent probes in bioanalysis, because of their unique spectral properties, photostability, and low-cost synthesis. We report for the first time the application of europium-doped gadolinium oxide (Eu:Gd_2O_3) nanoparticles to the optical imaging of antibody micropatterns. The nanoparticles were synthesized by spray pyrolysis and coated with antibody (IgG) molecules by physical adsorption. Our experiments showed that the Eu:Gd_2O_3 is a good biocompatible solid support for antibody immobilization. The antibodies (anti-rabbit IgG) immobilized on the nanoparticles had excellent biological activity in the specific recognition reaction with rabbit IgG patterned in line strips (10 μm×10 μm) on a glass substrate by use of a microcontact printing technique. The specific immunoreaction was confirmed by two independent microscopic techniques—fluorescence and scanning electron microscopy (SEM). Both microscopic images revealed that the nanoparticles were organized into designated structures as defined by the microcontact printing process with negligible non-specific binding. The nanoparticles can be used as fluorescent markers in a variety of immunosensing applications in a microscale format.

Keywords Nanoparticles · Lanthanide oxide · Fluorescence · Immunoassay · Microarray · Microcontact printing

M. Nichkova (✉) · S. J. Gee · B. D. Hammock
Department of Entomology, University of California Davis,
One Shields Avenue,
Davis, CA 95616, USA
e-mail: mnichkova@ucdavis.edu
Tel.: +1-530-7526571
Fax: +1-530-7521537

D. Dosev · R. Perron · I. M. Kennedy
Department of Mechanical and Aeronautical Engineering,
University of California Davis,
One Shields Avenue,
Davis, CA 95616, USA

Introduction

Lanthanide luminescence detection has been established as a powerful approach in bioassays in recent years [1]. Lanthanide oxides are commonly used as luminescent materials in the lighting industry [2, 3]. Like lanthanide chelates [4], nanoparticles of lanthanide oxides have large Stokes shifts, narrow line-shaped emission bands, and long-lived luminescence (approximately 1–2 ms). They also have inherent photostability. In contrast with semiconductor quantum dots [5, 6], the emission wavelength of the oxide nanoparticles is independent of particle size and hence monodispersity is less crucial, leading to lower synthesis costs. Surface modification does not, furthermore, significantly affect their optical properties, because their luminescence arises as a result of electronic transitions of the lanthanide ion. Oxide nanoparticles lack photoblinking, because of the large number of luminescent ions in one nanoparticle.

Many methods have recently been proposed for synthesis of lanthanide oxide nanoparticles [7–11]. One is spray pyrolysis, which is quick, simple, scalable for mass production, and environmentally friendly [12, 13]. It also enables a choice between different combinations of host and doping materials. Gd_2O_3 is known to be an excellent host material for doping with Eu^{3+} ions [14]. Although the physical properties (luminescence, doping, etc.) of lanthanide oxide nanoparticles have been extensively studied, there are only a few reports on their biological application [15, 16]. Crystalline europium oxide (Eu_2O_3) nanoparticles, have been used as a fluorescent label in a competitive immunoassay with magnetic separation for the herbicide atrazine; the detection limit was comparable to that of the respective enzyme-linked immunosorbent assay (ELISA) [15]. Here we propose the use of Eu^{3+}-doped gadolinium oxide nanoparticles (Eu:Gd_2O_3) as reporters for optical detection and visualization of antibody arrays.

Protein microarray technology is a powerful tool for identification, quantification, and functional analysis of proteins [17, 18]. It is of major interest for proteomic

research in basic and applied biology and for diagnostic applications. Microcontact printing (μCP) is a relatively new method of chemically and molecularly patterning surfaces on a submicrometer scale [19]. Patterning of antibodies on to a variety of substrates by direct microcontact printing, and their antigen-binding capabilities, have been demonstrated [20–22]. The low cost of fabrication and the simplicity of transferring antibodies to substrates, compared with other techniques such as ink-jet printers, lithography, etc., makes μCP-fabricated arrays very attractive [23].

Although microarrays are usually visualized and analyzed using organic fluorescent dyes [21], their poor photostability, reduced quantum yields on conjugation to biomolecules, and self-quenching at high labeling ratios limit their effectiveness in such applications. New fluorescent probes for microarray-based bioanalysis that have high photochemical stability and can withstand numerous illumination cycles are highly desirable. Extended integration times would result in improved signal-to-noise ratios, enhanced sensitivity, better quantitation, and increased assay reliability. To improve the sensitivity of microarrays new reporter schemes using europium chelates [24], fluorophore-loaded latex beads [25], and inorganic nanocrystals (quantum dots) [26, 27] have been studied. We have recently demonstrated the suitability of Eu:Gd_2O_3 nanoparticles as fluorophores for visualization of protein micropatterns for the avidin–biotin system [28]. We now report the application of those nanoparticles to the optical detection of antibody micropatterns.

Experimental

Chemicals and materials

Anti-rabbit IgG (whole molecule, developed in goat), rabbit IgG, sheep IgG, and bovine serum albumin (BSA) were obtained from Sigma. Fluorescein isothiocyanate (FITC) was purchased from Aldrich. BCA protein assay kit was obtained from Pierce. Rabbit IgG-fluorescein was prepared by a conjugation reaction between the amine groups of the protein and FITC, in accordance with a standard procedure recommended by Molecular Probes [29]. The amount of labeling obtained for rabbit IgG-fluorescein was 6 mol fluorescein mol^{-1} IgG. Phosphate-buffered saline (PBS) (pH=7.5) was 10 mmol L^{-1} phosphate buffer, 0.8% saline. Black 96-well plates from Nunc were used for fluorescence measurements. Clay Adams cover glass from Fisher Scientific (Pittsburgh, PA, USA) was used as the substrate for microcontact printing of proteins and fluorescence characterization, and a n-doped Si wafer was used for SEM characterization. The polydimethylsiloxane (PDMS) stamp was prepared in accordance with a literature method [30], using Sylgard 184 silicon elastomer (Dow Corning, Midland, MI, USA). The stamp used in the microcontact printing had a patterned matrix (1 cm^2) of 10 μm×10 μm strips.

Instrumentation

The size and the morphology of the Eu:Gd_2O_3 nanoparticles were determined by using a Philips CM-12 transmission electron microscope (TEM). Fluorescence measurements were performed on a Spectramax M2 cuvette/microplate reader (Molecular Devices, Sunnyvale, CA, USA). A VWR (Brisbane, CA, USA) 75 D ultrasonic bath was used for treating the nanoparticle suspensions and for cleaning procedures. Fluorescent images were acquired with a Leica TCS-SP laser scanning confocal microscope equipped with UV, argon, krypton, and helium–neon lasers for excitation and photomultiplier tubes (PMT) for detection. Leica confocal software LCS Lite 2.0 was used for image acquisition. A laser beam at 488 nm was used for excitation of the Eu:Gd_2O_3 nanoparticles. An FEI XL30-SFEG scanning electron microscope was used for SEM characterization.

Coating of Eu:Gd_2O_3 nanoparticles with antibody

Eu:Gd_2O_3 nanoparticles (1 mg) were suspended, by use of an ultrasonic bath, in 1 mL 25 mmol L^{-1} phosphate buffer, pH=7 in a polypropylene tube previously coated with 0.5% BSA to avoid loss of antibody to the tube walls. A solution of 2 mg mL^{-1} antibody (anti-rabbit and/or sheep IgG) were added to the particle suspension and incubated in a rotating mill overnight at room temperature. The suspension was then centrifuged at 15,000×*g* for 5 min. The supernatant was discarded and the nanoparticle pellet was resuspended in the same buffer to wash off the excess protein. This procedure was repeated three times. Efficient separation of free IgG was ensured by monitoring the concentration of protein in the supernatant solution after each wash using the BCA protein assay kit. To ensure there was no bare particle surface left, the antibody-coated Eu:Gd_2O_3 nanoparticles were incubated in 1 mL 0.5 mg mL^{-1} BSA solution in 25 mmol L^{-1} phosphate buffer for 1 h at room temperature in the rotating mill. After three consecutive washes by centrifugation and resuspension in fresh buffer the nanoparticles were used for the micropattern detection assays.

Quantification of the active binding sites on the surface of the antibody-coated Eu:Gd_2O_3 nanoparticles

The number of active binding sites on the surface of the anti-rabbit IgG-Eu:Gd_2O_3 nanoparticles was determined by using rabbit IgG labeled with fluorescein (IgG-fluorescein) and measuring the fluorescein fluorescence from the particle-bound labeled rabbit IgG. The nanoparticles were incubated in a rotating mill for 2 h with 100 μg mL^{-1} IgG-fluorescein in PBST buffer. The particle-bound IgG-fluorescein was separated from free labeled IgG by centri-

fugation then three cycles of washes and resuspension. Negative controls were prepared by exchanging the anti-rabbit IgG with sheep IgG in the coating procedure. Samples were run in duplicate. A standard plot of IgG-fluorescein in carbonate–bicarbonate buffer in the presence of the same amount of non-coated nanoparticles was used for quantification of the number of active binding sites on the nanoparticle surface.

Microcontact printing of rabbit IgG. Substrate, stamp, and sample preparation

Cover glass was used as the solid substrate for microcontact printing of antibodies and the consecutive specific interactions. Before use the substrate was thoroughly washed in an ultrasonic bath in acetone, ethanol, and deionized water, for 10 min each, then dried under a gentle stream of nitrogen. The PDMS stamp was washed by sonication in ethanol (3×10 min), dried under nitrogen, and exposed to a solution of the inking protein (50 μg mL^{-1} rabbit IgG in PBS) for 40 min. Excess solution was removed, and the stamp was dried under a stream of nitrogen gas. After inking, the stamp was brought into contact with the glass substrate and a very small amount of force was applied to make good contact between both surfaces. The stamp was removed after 2 min and the substrate was rinsed with PBS and deionized water and dried under nitrogen. The uncovered areas on the glass substrate were blocked with 2 mg mL^{-1} BSA solution in PBS for 1 h. After washing and drying the glass was incubated with a suspension of the anti-rabbit IgG-coated Eu:Gd_2O_3 nanoparticles in carbonate–bicarbonate buffer for 1 h in a shaker, enabling specific interaction to occur. The substrate was finally rinsed with buffer and water and then dried under nitrogen.

Results and discussion

Luminescent Eu:Gd_2O_3 nanoparticles

Luminescent Eu^{3+}-doped Gd_2O_3 (Eu:Gd_2O_3) nanoparticles were synthesized by spray pyrolysis in accordance with our previously reported procedure [13, 31]. The nanoparticles obtained have dense morphology and approximately spherical shape. Particles in the size range 5–200 nm with an average diameter of 120 nm were isolated by centrifugation. Their luminescence can be excited in different wavelength ranges: 250–280 nm, 350–400 nm, and 460–500 nm. On excitation the Eu:Gd_2O_3 nanoparticles emit a bright red peak centered at 612 nm with a full-width half-maximum (FWHM) of 5 nm which is very narrow in comparison with other fluorophores. The fluorescence lifetime of the nanoparticles is approximately 1 ms, enabling time-resolved measurements [32].

The doping concentration of Eu^{3+} in the host Gd_2O_3 is of key importance for the fluorescence lifetime and intensity of the Eu:Gd_2O_3 nanoparticles [9, 10]. The possibility of precise control of this concentration is one of the advantages of the spray pyrolysis method. At high doping concentrations it is possible self-quenching to occur, because of non-radiative energy transfer between different Eu^{3+} ions. If the doping concentration is too low, however, there will not be enough emitting centers and the fluorescence intensity will be low [9]. Thus, with the objective of optimizing the photoluminescence of the particles we synthesized Eu:Gd_2O_3 nanoparticles with different Eu^{3+} doping concentrations (5, 10, 15, 20, 25, 30, and 100% corresponding to pure Eu_2O_3). A colloidal suspension containing 10 μg particles in 100 μL deionized water was prepared for each doping and the fluorescence spectra were measured on a plate reader equipped with a pulsed xenon lamp for excitation and a photomultiplier tube (PMT) for detection. The excitation wavelength was set at 260 nm. The detection start time was set at 50 μs after the excitation, to reduce the background signal, and the detection end time was at 1,500 μs, to take all the emitted photons into account. The fluorescence spectra of all the samples had identical features with the main peak centered at 612 nm, as shown in Fig. 1. The intensity of this peak was different for the different doping concentrations, however. The insert in Fig. 1 shows that the fluorescence intensity increased with doping from 5% up to 20%. For doping higher than 20%, the detected signal intensity decreased dramatically, because of concentration self quenching of Eu^{3+} ions, with the lowest levels found for the pure Eu_2O_3 sample. On the basis of these results, we chose 20% doping for further application in immunodetection schemes. Here we must note that this was an optimum doping concentration in the context of our particular synthesis process. Because of the rapid temperature quenching that particles experience in flame-spray pyrolysis, phase segregation (i.e. formation of Eu_2O_3 clusters in the Gd_2O_3 matrix) is very unlikely, and this enables the relatively high doping ratio to be achieved.

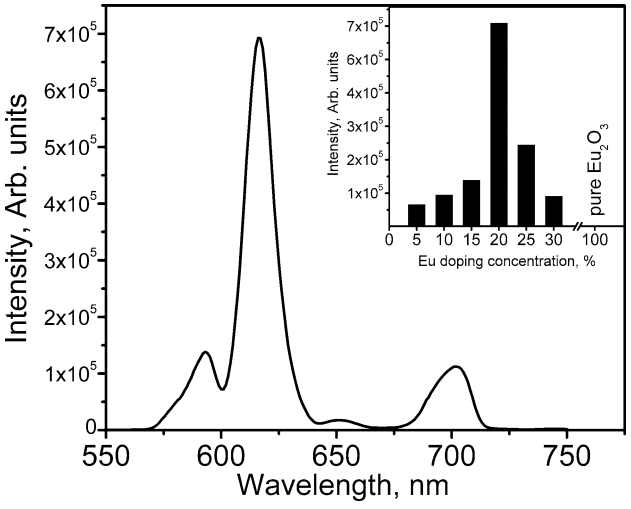

Fig. 1 Fluorescence spectrum of Eu:Gd_2O_3 nanoparticles excited at 260 nm. The *insert* shows the fluorescence intensity of the main emission peak at 612 nm for different doping concentrations

Coating the Eu:Gd_2O_3 nanoparticles with antibodies

The spontaneous physical adsorption of proteins on to nanoparticle surfaces because of hydrophobic and/or electrostatic forces has been reported for dye-doped silica nanoparticles [33], silole nanocrystals [34, 35], and quantum dots [36–39]. In our previous work we have successfully used the direct-coating method for biofunctionalization of Eu:Gd_2O_3 nanoparticles with avidin [31]. This method is attractive, because it is a one-step procedure (chemical functionalization and conjugation steps are avoided), the adsorbed proteins retain their activity, the nanoparticle luminescence is not affected by the protein layer, and their surface can be efficiently blocked to avoid non-specific binding in bioassays. To use the luminescent Eu:Gd_2O_3 nanoparticles as labels for immunosensing we used the same approach for antibody functionalization.

We coated the Eu:Gd_2O_3 nanoparticles with antibodies (anti-rabbit IgG) by the procedure described in the Experimental section. TEM studies and detection of active binding sites on the surface of the nanoparticles suggested that adsorption of the IgG molecules was successful. In Fig. 2 a typical TEM image of a bare particle is compared with that of an IgG-coated nanoparticle. The bare particle is nearly uniformly dark and its contour is clear and highly contrasted. The IgG-coated particle, in contrast, has a dark center corresponding to Eu:Gd_2O_3 and a lighter shell corresponding to the IgG layer which has a "hairy", irregular shape with radial formations extending out of the particle surface. We have estimated the thickness of the protein shell is approximately 10 nm, similar to the dimensions of the IgG molecule (10 nm×14 nm×5 nm) [40, 41] and data reported on the formation of an IgG monolayer on the surface of polystyrene particles [42]. Assuming 120 nm average particle diameter and 100 nm^2 footprint of a single antibody molecule, we estimated that the surface of 1 mg nanoparticles would be completely covered by a ~56 pmol densely packed monolayer of IgG molecules.

The immunoreactivity of the anti-rabbit IgGs immobilized on the surface of the Eu:Gd_2O_3 nanoparticles was tested by interaction with rabbit IgG labeled with fluorescein. The number of active binding sites was determined by measuring the fluorescence of the rabbit IgG-fluorescein bound to the particles through the antibody–antigen interaction. Eu:Gd_2O_3 particles coated with sheep IgG under the same conditions were used as a negative control. The number of anti-rabbit IgG binding sites as a function of the amount of antibody used in the coating reaction is presented in Fig. 3. Saturation of ~75 pmol binding sites is achieved by use of 400 μg IgG mg^{-1} particles in the coating procedure. The experimentally determined binding sites are of the same order of magnitude as that theoretically estimated, which indicates formation of an IgG monolayer on the particle surface. The saturation conditions were selected for preparation of anti-rabbit IgG-functionalized Eu:Gd_2O_3 nanoparticles and their application to the fluorescence imaging of antibody micropatterns.

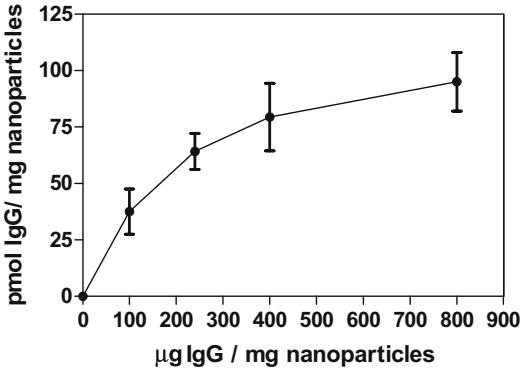

Fig. 3 Active antibody binding sites on the surface of the Eu:Gd_2O_3 nanoparticles as a function of the amount of antibody used in the coating procedure. Anti-rabbit IgG was adsorbed on the surface of the nanoparticles and the binding sites were detected by interaction with rabbit IgG-fluorescein

It should be noted that the number of binding sites on the surface of the nanoparticles can be controlled easily by varying the specific antibody concentration. This can be achieved by choosing a different ratio between specific and non-specific antibody (e.g. anti-rabbit IgG:sheep IgG) or blocking protein (e.g. anti-rabbit IgG:BSA) in the coating solution. The mechanism of antibody adsorption on the oxide surface is not yet fully understood. At low ionic strength electrostatic forces play a very important role in

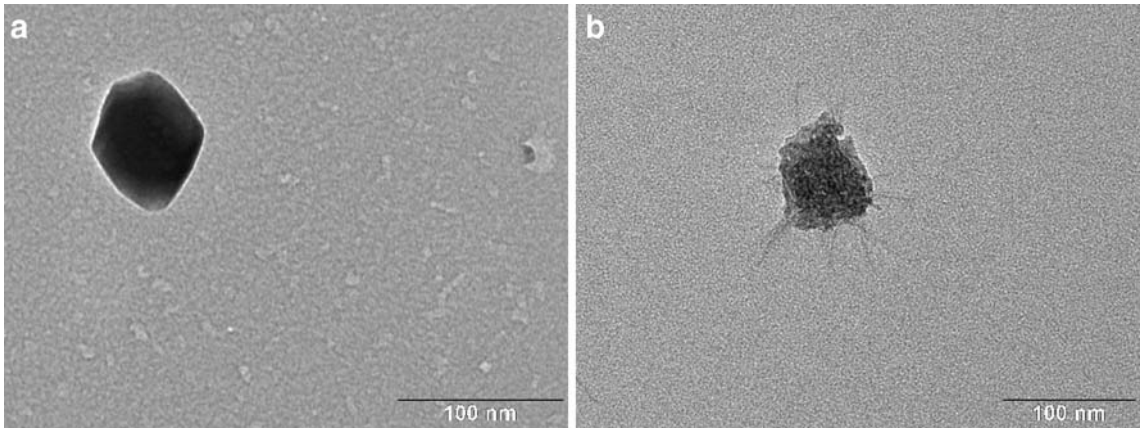

Fig. 2 TEM images of Eu:Gd_2O_3 nanoparticles: (**a**) non-coated nanoparticles; (**b**) antibody-coated nanoparticle

the adsorption mechanism. Given that the IgGs were readily adsorbed, electrostatic attraction between the nanoparticle surface and the antibodies affects adsorption of the antibodies. Other forces, for example hydrophobic interaction, van der Waals force, and H-bonding can also occur.

In addition to the biological activity of the adsorbed antibodies, the stability of the protein coating is another important issue for their application as fluorophor labels in immunoassays. We tested the stability of the IgG layer in some of the most commonly used buffers, for example PBS, phosphate, and carbonate buffers. After separation of the nanoparticles from the storage buffer by centrifugation, the protein concentration in the supernatant was determined by the BCA protein assay. The IgG coating layer of the nanoparticles was stable at 4°C for 2 months. Weekly check of binding sites on the particle surface showed deviation from the initially detected number within a range of ±10%, which we attribute to experimental error rather than to a change in the number of binding sites.

Fluorescence imaging of rabbit IgG micropatterns with anti-rabbit IgG–Eu:Gd_2O_3 nanoparticles

The antibody-functionalized Eu:Gd_2O_3 nanoparticles were used as fluorescent reporters in the anti-rabbit/rabbit IgG immunoreaction. Rabbit IgG micropatterns (10 μm×10 μm) were prepared on glass substrates by the μCP technique (Fig. 4a). To avoid possible non-specific binding the bare glass surface was blocked with BSA (Fig. 4b). Interaction between the immobilized rabbit IgGs and the anti-rabbit IgG-coated Eu:Gd_2O_3 nanoparticles then occurred during incubation of the substrate with the particle suspension (Fig. 4c). The pattern obtained was observed through a confocal fluorescence microscope. The image shown in Fig. 5 was obtained by 3D scanning of the micropattern and is a result of 96 scans in the vertical (*Z*) direction. Scanning laser emission at 488 nm was used to excite the Eu:Gd_2O_3 nanoparticles. The resulting image shows clear red strips formed by the Eu:Gd_2O_3 particles specifically bound by the antibody–antigen interaction and the dark empty spaces between the red strips corresponding to the BSA-blocked areas. The strips are 10 μm wide and reproduce the pattern of the PDMS stamp used in the μCP. The dark strips are an internal negative control and are indicative of negligible non-specific binding. These results show that adsorption of IgG on the Eu:Gd_2O_3 nanoparticles is an efficient method for their biofunctionalization that does not disturb the activity of the antibody. Blocking with BSA is an excellent way of preventing non-specific adsorption of the IgG-coated nanoparticles by the substrate surface. The intrinsic photostability of the Eu:Gd_2O_3 enables prolonged laser exposure and image acquisition. The fluorescent pattern did not suffer photobleaching during the observation process, which indicates the suitability of Eu:Gd_2O_3 nanoparticles as fluorescent labels with extended excitation periods.

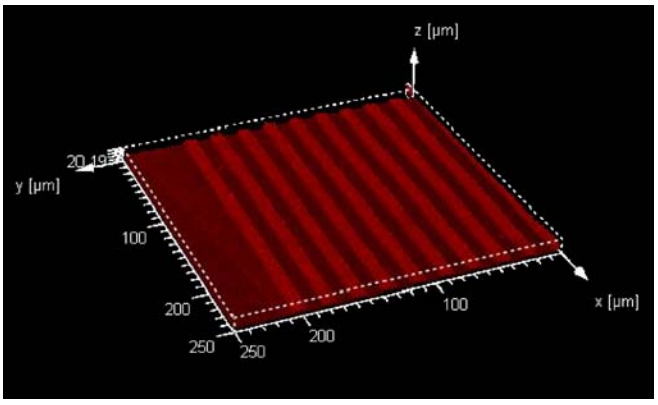

Fig. 5 Fluorescence image of specifically immobilized anti-rabbit IgG-Eu:Gd2O3 nanoparticles on printed rabbit IgG

SEM characterization of the antibody micropatterns

For more detailed studies at the single nanoparticle level the antibody micropatterns were characterized by scanning electron microscopy (SEM). For this purpose, the micropatterns were prepared on a silicon wafer instead of glass

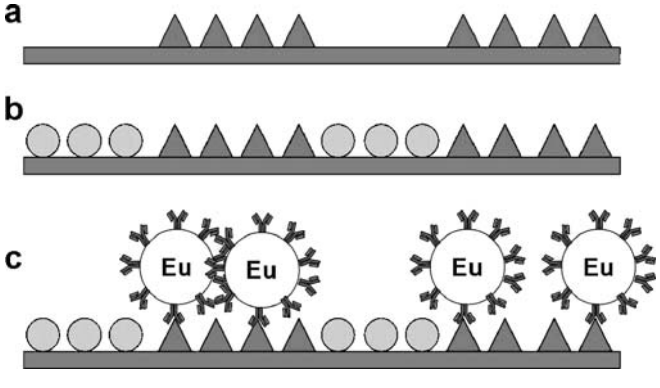

Fig. 4 Principle of the microimmunoassay using Eu:Gd_2O_3 as biolabels: (**a**) microcontact printing of rabbit IgG; (**b**) blocking with BSA; (**c**) specific immunoreaction between the patterned rabbit IgG and the anti-rabbit IgG-coated Eu:Gd_2O_3 nanoparticles

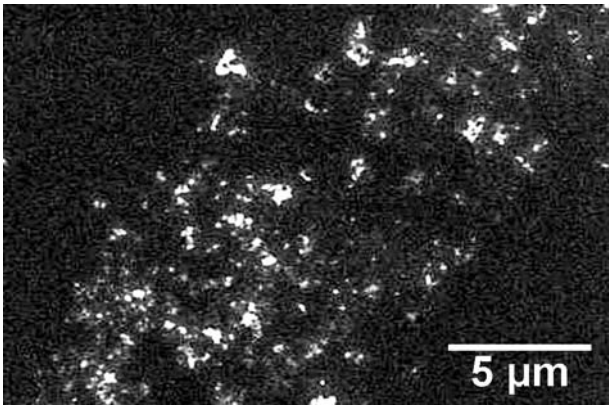

Fig. 6 Scanning electron microscopy image of specifically immobilized anti-rabbit IgG-Eu:Gd_2O_3 nanoparticles on printed rabbit IgG

slide but following the procedure described above and keeping all the experimental conditions identical. Use of the silicon wafer ensured a perfectly flat surface and conductivity of the substrate—conditions required for the SEM studies. The SEM image presented in Fig. 6 illustrates a segment of a strip formed by the specifically bound nanoparticles. The size of the smallest particles that can be individually distinguished as white spots on the dark background is approximately 100 nm. Particles smaller than this are visible as grey clouds. It is apparent that some areas within the strip are more densely populated with particles than others. A similar effect was observed by other authors when immobilizing polystyrene beads by specific avidin–biotin binding [43]. In our work this non-uniform distribution of the immobilized nanoparticles within the strip can be attributed to inefficient antibody–antigen binding, because of steric hindrance, partial aggregation, and/or poor diffusion of the particles near the substrate during the incubation. The density of surface coverage could be improved by further optimization of the coating of the nanoparticles, substrate incubation, and the washing procedures. Despite this, the particles are arranged in a good match with the printed patterns. Only a few individual particles can be observed in the areas blocked with BSA, showing non-specific binding is very low.

Conclusions

This is the first demonstration that luminescent nanoparticles made from lanthanide oxides can be successfully used to visualize antibody micropatterns. The unique spectral properties, photostability, and low price of synthesis of these novel materials make them an attractive alternative to other widely used fluorophores. The surface properties of the Eu:Gd_2O_3 nanoparticles presented in this paper enable easy one-step bio-functionalization of the particles with IgG molecules. Antibody-functionalized Eu:Gd_2O_3 nanoparticles can be used as reporters in a variety of immunodetection systems in the array format presented here with potential application in biosensor development and proteomics studies. Further optimization of nanoparticle biofunctionalization is needed, in particular with regard to efficient antibody orientation and avoidance of aggregation. Application of this detection approach to quantitative analysis of proteins and small molecules in microimmunoassays is currently under study in our laboratory.

Acknowledgements The authors wish to acknowledge the support of the National Science Foundation, grant DBI-0102662, the Superfund Basic Research Program with Grant 5P42ES04699 from the National Institute of Environmental Health Sciences NIH, and the support of the Cooperative State Research, Education, and Extension Service, US Department of Agriculture, under Award No. 05-35603-16280.

References

1. Steinkamp T, Karst U (2004) Anal Bioanal Chem 380:24–30
2. Bhargava RN (1996) J Lumin 70:85–94
3. Tissue BM (1998) Chem Mater 10:2837–2845
4. Diamandis EP, Christopoulos TK (1990) Anal Chem 62: 1149A–1157A
5. Chan WCW, Maxwell DJ, Gao XH, Bailey RE, Han MY, Nie SM (2002) Curr Opin Biotechnol 13:40–46
6. Riegler J, Nann T (2004) Anal Bioanal Chem 379:913–919
7. Eilers H, Tissue BM (1996) Chem Phys Lett 251:74–78
8. Hao J, Studenikin SA, Cocivera M (2001) J Lumin 93:313–319
9. Kang YC, Park SB, Lenggoro IW, Okuyama K (1999) J Phys Chem Solids 60:379–384
10. Bazzi R, Flores-Gonzalez MA, Louis C, Lebbou K, Dujardin C, Brenier A, Zhang W, Tillement O, Bernstein E, Perriat P (2003) J Lumin 102–103:445–450
11. Bian L-j, Xi H-a, Qian X-f, Yin J, Zhu Z-k, Lu Q-h (2002) Mater Res Bull 37:2293–2301
12. Kang YC, Roh HS, Park SB, Park HD (2002) J Mater Sci Lett 21:1027–1029
13. Dosev D, Guo B, Kennedy IM (2005) Journal of Aerosol Science, in press, available on-line at http://www.sciencedirect.com
14. Gordon WO, Carter JA, Tissue BM (2004) J Lumin 108:339–342
15. Feng J, Shan GM, Maquieira A, Koivunen ME, Guo B, Hammock BD, Kennedy IM (2003) Anal Chem 75:5282–5286
16. Beaurepaire E, Buissette V, Sauviat MP, Giaume D, Lahlil K, Mercuri A, Casanova D, Huignard A, Martin JL, Gacoin T, Boilot JP, Alexandrou A (2004) Nano Lett 4:2079–2083
17. Espina V, Mehta AI, Winters ME, Calvert V, Wulfkuhle J, Petricoin EF, Liotta LA (2003) Proteomics 3:2091–2100
18. Kusnezow W, Hoheisel JD (2002) Biotechniques:14− +
19. Kane RS, Takayama S, Ostuni E, Ingber DE, Whitesides GM (1999) Biomaterials 20:2363–2376
20. Tan JL, Tien J, Chen CS (2002) Langmuir 18:519–523
21. Bernard A, Renault JP, Michel B, Bosshard HR, Delamarche E (2000) Adv Mater 12:1067–1070
22. Graber DJ, Zieziulewicz TJ, Lawrence DA, Shain W, Turner JN (2003) Langmuir 19:5431–5434
23. Lin SC, Tseng FG, Huang HM, Huang CY, Chieng CC (2001) Fresenius J Anal Chem 371:202–208
24. Scorilas A, Bjartell A, Lilja H, Moller C, Diamandis EP (2000) Clin Chem 46:1450–1455
25. Orth RN, Clark TG, Craighead HG (2003) Biomed Microdevices 5:29–34
26. Geho D, Lahar N, Gurnani P, Huebschman M, Herrmann P, Espina V, Shi A, Wulfkuhle J, Garner H, Petricoin E, Liotta LA, Rosenblatt KP (2005) Bioconjug Chem 16:559–566
27. Gerion D, Chen FQ, Kannan B, Fu AH, Parak WJ, Chen DJ, Majumdar A, Alivisatos AP (2003) Anal Chem 75:4766–4772
28. Dosev D, Nichkova M, Liu M, Guo B, Liu GY, Hammock BD, Kennedy IM (2005) Journal of Biomedical Optics, 10 (6):064006-1–064006-7
29. (http://www.probes.com) Molecular Probes, Amine-reactive Probes
30. Kumar A, Whitesides GM (1993) Appl Phys Lett 63:2002–2004
31. Dosev D, Nichkova M, Liu M, Liu G-y, Hammock BD, Kennedy IM (2005) Proceedings SPIE - The International Society for Optical Engineering, Biomedical Optics, BIOS, San Jose, CA, 2005. 5699:473–481
32. Shi-Che C, Peron R, Dosev D, Kennedy IM (2004) SPIE Proceedings, BioMEMS and Nanotechnology 5275:186–196
33. Tapec R, Zhao XJJ, Tan WH (2002) J Nanosci Nanotechnol 2:405–409
34. Chan CPY, Bruemmel Y, Seydack M, Sin KK, Wong LW, Merisko-Liversidge E, Trau D, Renneberg, R (2004) Anal Chem 76:3638–3645

35. Chan CP-y, Haeussler M, Zhong TB, Dong Y, Sin K-k, Mak W-c, Trau D, Seydack M, Renneberg R (2004) J Immunol Methods 295:111–118
36. Mattoussi H, Mauro JM, Goldman ER, Anderson GP, Sundar VC, Mikulec FV, Bawendi MG (2000) J Am Chem Soc 122:12142–12150
37. Goldman ER, Anderson GP, Tran PT, Mattoussi H, Charles PT, Mauro JM (2002) Anal Chem 74:841–847
38. Goldman ER, Balighian ED, Mattoussi H, Kuno MK, Mauro JM, Tran PT, Anderson GP (2002) J Am Chem Soc 124:6378–6382
39. Gao XH, Chan WCW, Nie SM (2002) J Biomed Opt 7:532–537
40. Silverton EW, Navia MA, Davies DR (1977) Proceedings of the National Academy of Sciences of the United States of America 74:5140
41. Amit AG, Mariuzza RA, Phillips SE, Poljak RJ (1986) Science 233:747
42. Caruso F, Mohwald H (1999) J Am Chem Soc 121:6039–6046
43. Andersson H, Jonsson C, Moberg C, Stemme G (2002) Talanta 56:301–308